used are important. Previous estimates of parasite diversity were restricted by DNA sequence availability and used a limited number of genes and/or sequences from GenBank. Databases frequently contain erroneous DNA sequences[23], and it is difficult to verify the accuracy of the sequences and the identities of the parasites from which they were obtained. Although synonymous sites and non-coding sequences are assumed to be relatively neutral, the degree of deviation from neutrality may not be the same for genes under various selection pressures. Most of the genes used in previous studies[1,2] are immune/drug targets or housekeeping genes that could be under strong selection.

In contrast, we have used a large number of SNPs and parasites of highly diverse genetic background to estimate the divergence time and effective population size. We have shown that the *P. falciparum* population is quite ancient and diverse, a result that will be important in the development of drugs and vaccines. □

## Methods

### Gene sequences and parasite DNA

Predicted coding sequences of the 3D7 parasite were downloaded from PlasmoDB (http://www.plasmodb.org). Coding sequences were defined according to annotation in the database. The whole gene sequence, including any introns, was also obtained for sequence alignment. Introns were identified by sequence alignment of predicted coding sequences and the genomic DNA sequence. Parasite culture and DNA extraction were as described[24].

### Amplification of parasite DNA and DNA sequencing

Two to six primers were designed to amplify and sequence DNA fragments up to 1.5 kb from each of 215 predicted genes on chromosome 3, excluding multigene families such as *rifin*, *var*, *stevo* and *clag*[13]. PCR set-ups contained 4 μl DNA (~5 ng), 0.3 μl of each primer (100 μM), and 45 μl of PCR mix containing 5 μl 10× PCR buffer, 1.0 μl dNTPs (10 mM), and 0.2 μl (5 U $\mu l^{-1}$) *Taq* polymerase (Roche Applied Science). All amplifications were performed with one cycling condition: 94 °C for 2 min, 35 cycles of 94 °C for 20 s, 52 °C for 10 s, 48 °C for 10 s, and 60 °C for 1.5 min. The PCR product was treated with 2 μl ExoSAP-IT (USB) at 37 °C for 15 min and 80 °C for another 15 min. 5 μl of the treated product was used in sequencing reaction with dichlororhodamine or BigDye terminator chemistry on an ABI377 or ABI3100 DNA sequencer (Applied Biosystem).

### Data analysis

DNA sequences were aligned using Sequencher 3.1 (Gene Codes Corp.). All potential SNPs and discrepancies were verified by visual inspection. The DnaSP program[25] was used to calculate $\pi$, $\theta$, and other parameters for each gene. The neutrality test was done using the codonml program of the software package PAML[17]. Estimates of nucleotide substitution rates, divergence time, and population size were made using methods described elsewhere[1,2,5]. To obtain LCR from the genes, we first corrected for the background amino-acid composition bias by randomly shuffling all the residues and determined the trigger complexity that results in 4% of the database being within LCR[26] (J. C. Wootton and O.H.B., manuscript in preparation). We then used this trigger complexity to run the SEG program[21].

Received 21 January; accepted 24 April 2002; doi:10.1038/nature00836.


1. Rich, S. M., Licht, M. C., Hudson, R. R. & Ayala, F. J. Malaria's Eve: evidence of a recent population bottleneck throughout the world populations of *Plasmodium falciparum*. *Proc. Natl Acad. Sci. USA* **95,** 4425–4430 (1998).
2. Volkman, S. K. *et al.* Recent origin of *Plasmodium falciparum* from a single progenitor. *Science* **293,** 482–484 (2001).
3. Hughes, A. L. & Verra, F. Ancient polymorphism and the hypothesis of a recent bottleneck in the malaria parasite *Plasmodium falciparum*. *Genetics* **150,** 511–513 (1998).
4. Hey, J. Parasite populations: the puzzle of *Plasmodium*. *Curr. Biol.* **9,** R565–R567 (1999).
5. Hughes, A. L. & Verra, F. Very large long-term effective population size in the virulent human malaria parasite *Plasmodium falciparum*. *Proc. R. Soc. Lond. B* **268,** 1855–1860 (2001).
6. Saul, A. Circumsporozoite polymorphisms, silent mutations and the evolution of *Plasmodium falciparum*. *Parasitol. Today* **15,** 38–40 (1999).
7. Escalante, A. A., Barrio, E. & Ayala, F. J. Evolutionary origin of human and primate malarias: evidence from the circumsporozoite protein gene. *Mol. Biol. Evol.* **12,** 616–626 (1995).
8. Walliker, D., Babiker, H. & Ranford-Cartwright, L. in *Malaria: Parasite Biology, Pathogenesis, and Protection* (ed. Sherman, I. W.) 235–252 (American Society for Microbiology, Washington DC, 1998).
9. Conway, D. J. *et al.* High recombination rate in natural populations of *Plasmodium falciparum*. *Proc. Natl Acad. Sci. USA* **96,** 4506–4511 (1999).
10. Anderson, T. J. *et al.* Microsatellite markers reveal a spectrum of population structures in the malaria parasite *Plasmodium falciparum*. *Mol. Biol. Evol.* **17,** 1467–1482 (2000).
11. Templeton, A. Out of Africa again and again. *Nature* **416,** 45–51 (2002).
12. Gardner, M. J. *et al.* Chromosome 2 sequence of the human malaria parasite *Plasmodium falciparum*. *Science* **282,** 1126–1132 (1998).
13. Bowman, S. *et al.* The complete nucleotide sequence of chromosome 3 of *Plasmodium falciparum*. *Nature* **400,** 532–538 (1999).
14. Cargill, M. *et al.* Characterization of single-nucleotide polymorphisms in coding regions of human genes. *Nature Genet.* **22,** 231–238 (1999).
15. Graur, D. & Li, W.-h. *Fundamentals of Molecular Evolution* (Sinauer, Sunderland, Massachusetts, 2000).
16. Su, X. *et al.* A genetic map and recombination parameters of the human malaria parasite *Plasmodium falciparum*. *Science* **286,** 1351–1353 (1999).
17. Yang, Z. PAML: a program package for phylogenetic analysis by maximum likelihood. *Comput. Appl. Biosci.* **13,** 555–556 (1997).
18. Hughes, A. L. Circumsporozoite protein genes of malaria parasites (*Plasmodium* spp.): evidence for positive selection on immunogenic regions. *Genetics* **127,** 345–353 (1991).
19. Musto, H., Romero, H., Zavala, A., Jabbari, K. & Bernardi, G. Synonymous codon choices in the extremely GC-poor genome of *Plasmodium falciparum*: compositional constraints and translational selection. *J. Mol. Evol.* **49,** 27–35 (1999).
20. Pizzi, E. & Frontali, C. Low-complexity regions in *Plasmodium falciparum* proteins. *Genome Res.* **11,** 218–229 (2001).
21. Wootton, J. C. Non-globular domains in protein sequences: automated segmentation using complexity measures. *Comput. Chem.* **18,** 269–285 (1994).
22. Wootton, J. C. *et al.* Genetic diversity and chloroquine selective sweeps in *Plasmodium falciparum*. *Nature,* **418,** 320–323.
23. Louis, A., Ollivier, E., Aude, J. C. & Risler, J. L. Massive sequence comparisons as a help in annotating genomic sequences. *Genome Res.* **11,** 1296–1303 (2001).
24. Su, X., Kirkman, L. A., Fujioka, H. & Wellems, T. E. Complex polymorphisms in an approximately 330 kDa protein are linked to chloroquine-resistant *P. falciparum* in Southeast Asia and Africa. *Cell* **91,** 593–603 (1997).
25. Rozas, J. & Rozas, R. DnaSP version 3: an integrated program for molecular population genetics and molecular evolution analysis. *Bioinformatics* **15,** 174–175 (1999).
26. Wootton, J. C. & Federhen, S. Statistics of local complexity in amino acid sequence databases. *Comput. Chem.* **17,** 149–163 (1993).
27. Yu, A. *et al.* Comparison of human genetic and sequence-based physical maps. *Nature* **409,** 951–953 (2001).
28. Swofford, D. L. *PAUP**. Phylogenetic Analysis Using Parsimony (*and other methods). Version 4 (Sinauer Associates, Sunderland, Massachusetts, 2000).
29. Posada, D. & Crandall, K. A. MODELTEST: testing the model of DNA substitution. *Bioinformatics* **14,** 817–818 (1998).



### Acknowledgements

We thank T. Anderson, A. Saul, K. Hayton and J. Ribeiro for critical reading of the manuscript, and B. Marshall for editorial assistance. We also thank J. Wootton for supporting O.H.B. This work was partially supported by the NIH (W.-H.L.).


### Competing interests statement

The authors declare that they have no competing financial interests.

Correspondence and requests for materials should be addressed to X.-z.S. (e-mail: xsu@niaid.nih.gov).

# Dendritic spikes as a mechanism for cooperative long-term potentiation

**Nace L. Golding*†, Nathan P. Staff† & Nelson Spruston**

*Department of Neurobiology and Physiology, Institute for Neuroscience, Northwestern University, 2153 North Campus Drive, Evanston, Illinois 60208-3520, USA*
*† These authors contributed equally to this work*

**Strengthening of synaptic connections following coincident pre- and postsynaptic activity was proposed by Hebb as a cellular mechanism for learning[1]. Contemporary models assume that multiple synapses must act cooperatively to induce the post-synaptic activity required for hebbian synaptic plasticity[2–5]. One mechanism for the implementation of this cooperation is action potential firing, which begins in the axon, but which can influence synaptic potentiation following active backpropagation into dendrites[6]. Backpropagation is limited, however, and action potentials often fail to invade the most distal dendrites[7–10]. Here we show that long-term potentiation of synapses on the distal dendrites of hippocampal CA1 pyramidal neurons does require cooperative synaptic inputs, but does not require axonal action potential firing and backpropagation. Rather, locally**

* Present address: Section of Neurobiology, University of Texas at Austin, Patterson Labs, Austin, Texas 78712, USA

**generated and spatially restricted regenerative potentials (dendritic spikes) contribute to the postsynaptic depolarization and calcium entry necessary to trigger potentiation of distal synapses. We find that this mechanism can also function at proximal synapses, suggesting that dendritic spikes participate generally in a form of synaptic potentiation that does not require postsynaptic action potential firing in the axon.**

Hebb's view of the malleable synapse[1] has gained tremendous experimental support. Repeated pairing of presynaptic stimulation with postsynaptic depolarization leads reliably to long-term potentiation (LTP) of excitatory postsynaptic potentials (EPSPs)[11–13]. Postsynaptic action potentials can provide the necessary depolarization at some dendritic synapses, via backpropagation from the axon into dendrites[6]. At the most distal synapses, however, this mechanism may be ineffective, because action potential amplitude decreases markedly between the axon and the distal dendrites, especially during the repetitive firing necessary to induce LTP[7–10]. An alternative postsynaptic signal could be provided by dendritically generated spikes, which are produced by activation of sodium and calcium channels by large synaptic potentials in hippocampal or cortical dendrites[14–20].

To test this idea, we activated synapses on the distal dendrites of CA1 pyramidal neurons by placing a stimulating electrode in stratum lacunosum-moleculare (SLM) of hippocampal slices prepared from mature rats (Methods). LTP was induced using a physiologically relevant stimulus[6,21] consisting of EPSPs (2–4 mV) stimulated in bursts of five and paired with three postsynaptic action potentials, repeated at the naturally occurring theta frequency (Methods; Fig. 1a and b). To investigate the role of backpropagating action potentials in this form of LTP, tetrodotoxin (TTX) was applied to the axon, soma, and proximal dendrites. This manipulation prevented action potential initiation and backpropagation during the theta-burst stimulus, without affecting evoked EPSPs.

LTP at distal synapses was not affected by blocking action potential firing with proximal application of TTX (proximal TTX; Fig. 1c). In addition, LTP was not prevented by somatic hyperpolarization or voltage clamp near the resting potential, manipulations that prevented action potential initiation but which should not prevent depolarization of the distal dendrites[22] (Fig. 1e). Although backpropagating action potentials were not required, LTP at distal synapses did require significant depolarization, as smaller EPSPs (0.5–1 mV, paired with action potential firing) did not produce LTP, indicating that multiple synapses must cooperate to produce sufficient postsynaptic depolarization[2–5]. LTP could be observed at proximal synapses (with the stimulating electrode placed in stratum radiatum, SR) when small EPSPs were paired with action potentials using the theta-burst protocol (Fig. 1d and e). Thus, synaptic inputs sufficient to trigger axonally initiated, backpropagating action potentials can account for the cooperativity of LTP at proximal, but not distal, synapses.

We proposed that EPSPs summating during theta-burst stimulation of SLM produced cooperative LTP owing to the occurrence of regenerative spikes initiated in the dendrites. To test this hypothesis, we limited dendritic spiking by blocking a subset of voltage-activated calcium channels, while preventing backpropagating action potentials with proximal application of TTX. A combination of 50 μM nickel and 10 μM nimodipine was used to block a fraction of the low-threshold and high-threshold channels (primarily T- and L-type channels, respectively). Blocking some calcium channels in this way reduced the average magnitude of LTP from an 85% increase to a 52% increase (Fig. 2a and b), suggesting that activation

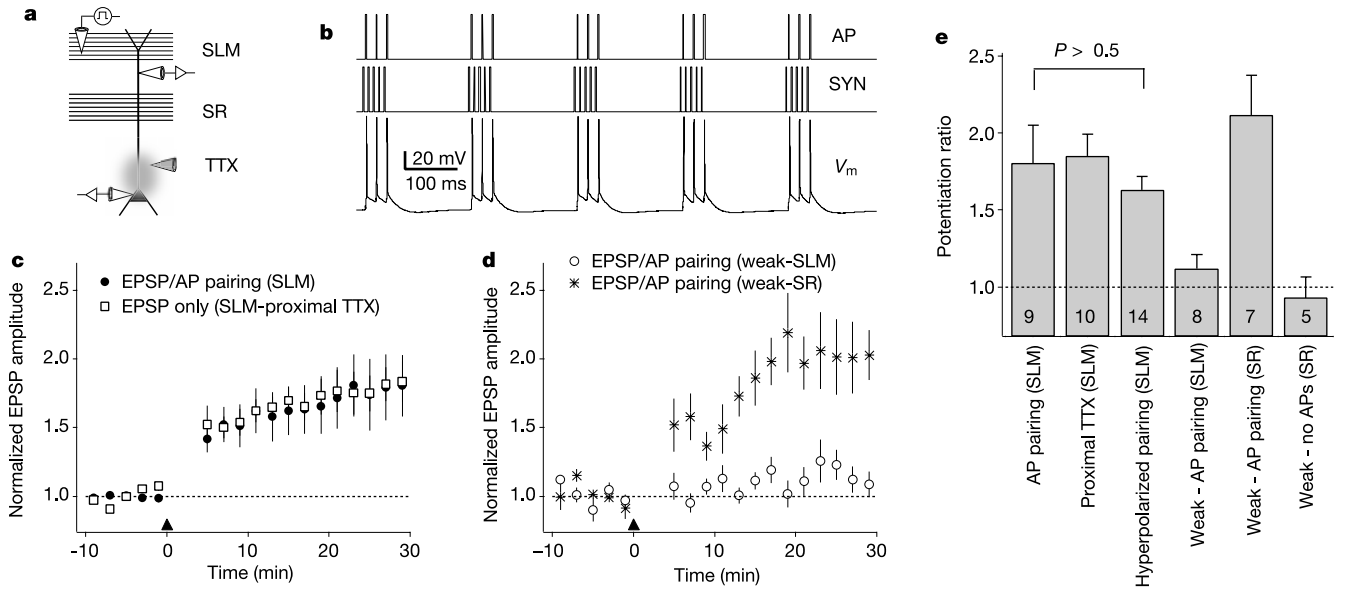


**Figure 1** Induction of long-term potentiation at distal synapses is independent of backpropagating action potentials. **a**, Recording configuration with whole-cell somatic patch-clamp recording, stimulation of stratum lacunosum-moleculare (SLM) axons, and application of 5 μM tetrodotoxin (TTX) near the soma to block action potentials in some experiments. SR, stratum radiatum. **b**, Theta-burst LTP induction protocol. Bursts of EPSPs (SYN; 5× synaptic stimulation at 100 Hz) were paired with triplets of action potentials (AP; 2-ms somatic current steps at 50 Hz). A single theta stimulus consisted of five EPSP/AP bursts at 5 Hz ($V_m$; one postsynaptic voltage response is shown). The theta stimulus was repeated 3 times, separated by 30 s. **c**, Normalized EPSP amplitude (2–4 mV) before and after theta-burst stimulation shows a similar degree of potentiation when induced with (filled circles) and without (proximal TTX, open boxes) the pairing of action potentials. **d**, Normalized EPSP amplitude (0.5–1 mV) before and after theta-burst stimulation. Weak stimulation paired with action potentials does not induce LTP at SLM synapses (open circles), but does at SR synapses (asterisks). **e**, Potentiation ratio (average EPSP 20–30 min after theta-burst stimulation to the average of the 10-min baseline) under various experimental conditions. Hyperpolarized pairing includes bursts paired with a 100-ms hyperpolarizing pulse (−1.0 to −1.5 nA) or somatic voltage clamp to the resting potential (about −65 mV). The number of experiments in each condition is indicated at bottom of each bar.

of voltage-gated calcium channels contributes to LTP at SLM synapses. A similar reduction in LTP was observed (from 85% increase to a 57% increase) when NMDA- (*N*-methyl-D-aspartate) type glutamate receptors were blocked by application of 50 μM AP5 and 20 μM MK-801 (Fig. 2a and b). Robust block of LTP was obtained when both NMDA receptors and a fraction of voltage-gated calcium channels were blocked together (Fig. 2a and b). In each of these experiments, the drugs were continuously present throughout the experiment, and baseline EPSP amplitude was set in the 2–4 mV range. There were no differences in the average baseline EPSP amplitude across the four groups. Separate experiments also indicated that these drugs did not affect peak amplitude or initial slope of individual EPSPs ($n = 3$, see Supplementary Information). The observed effects on LTP, however, suggest that bursts of EPSPs in SLM activate both NMDA receptors and calcium channels, which act synergistically to produce the local depolarization and calcium influx necessary to induce LTP.

To test further the hypothesis that the depolarization achieved during theta-burst stimulation was a critical determinant of co-operative LTP at SLM synapses, we examined the relationship between the magnitude of LTP and the change in somatic membrane potential ($V_m$) during the theta-burst stimulus (average peak $\Delta V_m$ during the 15 bursts used to induce LTP). Pooling the data for all four conditions (proximal TTX alone, or with partial calcium channel block, NMDA receptor block, or partial calcium channel and NMDA receptor block), a strong correlation emerged between the amount of depolarization and the magnitude of LTP (Fig. 2c). By contrast, no correlation was observed between the size of the baseline EPSP (2–4 mV) and the amount of LTP (Fig. 2d). These data suggest that EPSP summation and active responses during theta bursts are more important determinants of LTP than initial synaptic strength.

Sample traces during theta-burst stimuli are shown in Fig. 2e (examples from three experiments for each condition). Many of the responses exhibited signs of regenerative activity in the somatic recordings, despite the presence of somatically applied TTX. The only exception was when calcium channels and NMDA receptors were blocked together, in which case signs of regenerative activity were almost never observed (and there was less EPSP summation and little LTP). As the presence of regenerative events markedly increased the peak somatic depolarization during theta-burst stimulation, we proposed that these events contribute to the induction of LTP. Further, we postulated that these events were generated in the distal dendrites, where the activated synapses were located. To examine the correlation between these putative dendritic spikes and the induction of LTP, each experiment was analysed for the presence of regenerative events (rapid depolarizations greater than 3 mV above a sharp inflection point). Comparing experiments with and without putative dendritic spikes (filled and open symbols or bars in Figs 2c, d and f), much more LTP was observed when regenerative spikes were recorded in the soma than when they were absent.

To test directly the hypothesis that the somatic regenerative events reflected dendritically generated spikes, we performed simultaneous recordings from the soma and distal dendrites of CA1 neurons ($n = 6$; beyond 300 μm from the soma). Regenerative events were recorded in the dendrites during theta-burst stimulation of SLM (Fig. 3A). The largest of these events triggered somatic action potentials under normal conditions, but smaller events failed to trigger action potentials (Fig. 3A, a). When TTX was applied locally to the soma and proximal dendrites, dendritic spikes were always much larger than the correlated events in the soma (Fig. 3A,

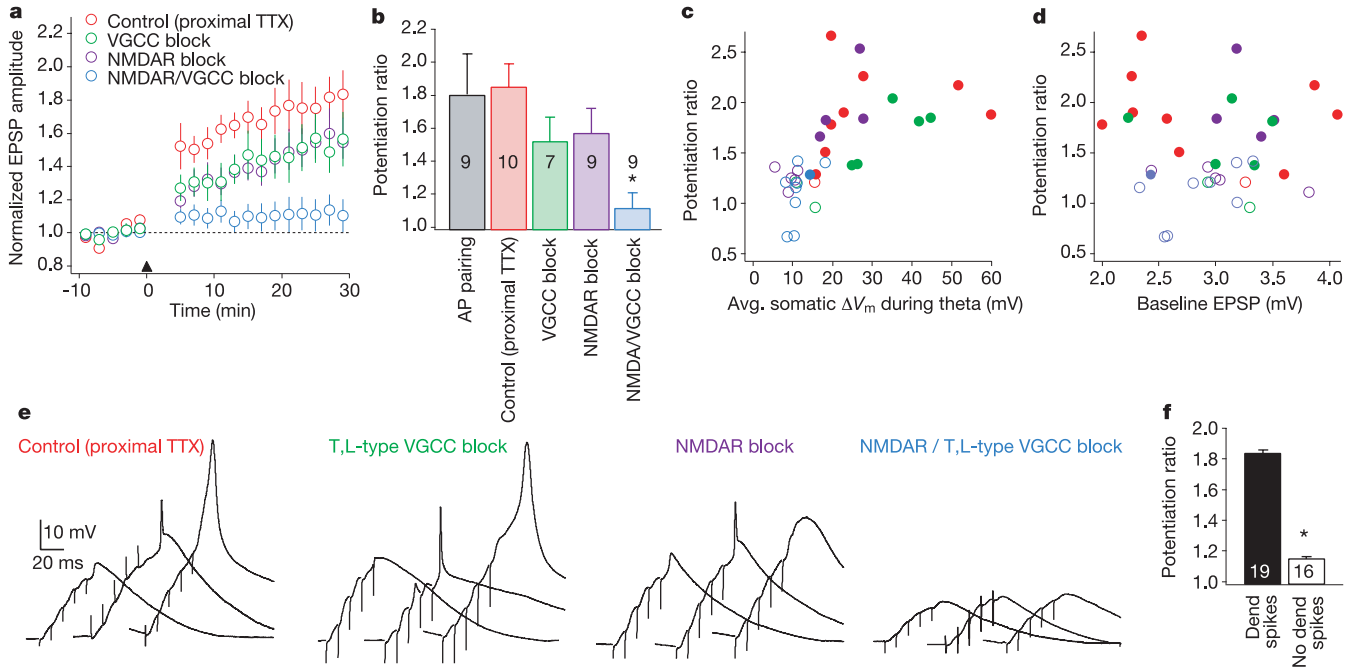


**Figure 2** LTP at distal synapses requires voltage-gated calcium channels and NMDA receptors. **a**, Normalized EPSP amplitude in response to SLM stimulation before and after theta-burst stimulus under different pharmacological conditions. Action potentials were always suppressed with proximal TTX application. Conditions: control (proximal TTX alone), NMDA receptor (NMDAR) blockade with 50 μM AP-5 and 20 μM MK-801, blockade of T- and L-type calcium channels (VGCC) with 50 μM $NiCl_2$ and 10 μM nimodipine, and combined block of both NMDA receptors and T- and L-type calcium channels. **b**, Potentiation ratios induced by theta-burst stimuli applied to SLM in the different pharmacological conditions (asterisk, $P < 0.05$; the number of experiments for each condition is indicated for each bar). **c**, Magnitude of LTP is correlated with the amplitude of the theta-burst stimulus response at the soma ($r = 0.62$; $P < 0.0001$). Symbols indicate cells where dendritic spikes were (filled) or were not (open) observed at the soma. **d**, Magnitude of LTP is not correlated with the amplitude of the baseline EPSP over a range spanning 2–4 mV ($r = -0.03$). Symbols as in **c**. **e**, Examples of theta-burst stimulus responses in the different pharmacological conditions. Spikes are apparent in all conditions except the combined NMDA receptor and calcium channel blockers. **f**, Magnitude of LTP is significantly greater in cells exhibiting dendritic spikes recorded at the soma as compared to those without visible dendritic spikes ($P < 10^{-6}$).

b)[15,17,23]. These double recordings show that the small regenerative events recorded in the soma correspond to larger, dendritically generated events that propagate poorly toward the soma. The correlation between these regenerative events and LTP strongly suggests that dendritic spikes contribute to LTP induction (Fig. 2c, d and f). Furthermore, dendritic spikes were sometimes present even when the somatic recording showed no obvious signs of regenerative activity. Such events may contribute to the LTP that was sometimes observed when no dendritic spikes were apparent in the somatic recording (Fig. 2c, d and f).

The contribution of dendritic spikes to distal dendritic depolarization and calcium entry was studied further using calcium imaging experiments. We compared the amplitude of distal dendritic calcium transients in SLM produced by a single burst of EPSPs just below and just above threshold for dendritic spikes detected at the soma (Fig. 3B, a–c). Despite the fact that these EPSPs were almost identical before the dendritic spike (Fig. 3B, b), the average calcium transient elicited with dendritic spikes apparent at the soma was 2.63 ± 0.45 times that without dendritic spikes ($n = 6$ cells; range 1.47–4.25; Fig. 3B, c). In contrast to the large calcium transients evoked by dendritic spikes, triplets of backpropagating action potentials did not evoke calcium transients above the noise in the distal dendrites of any of the five cells tested (for example, Fig. 3B, c). These findings suggest that large, dendritically initiated spikes produce much greater depolarization and calcium entry in distal CA1 dendrites than synaptic potentials (either alone or possibly with smaller dendritic spikes not detected at the soma) or backpropagating action potentials.

Taken together, our results strongly implicate dendritically generated spikes as key events in the induction of LTP at distal synapses on CA1 neurons, where action potential backpropagation is limited and does not affect LTP. We asked further whether dendritic spikes could also induce LTP at more proximal synapses on CA1 neurons. To test this idea, we induced LTP by stimulating SR strongly during the theta bursts while applying TTX onto the axon, soma, and proximal dendrite to prevent action potential initiation during theta-burst stimulation. Robust LTP was observed under these conditions, and regenerative activity clearly had its origin in the dendrite ($n = 4$, Fig. 4).

Voltage-gated calcium channels and NMDA receptors act synergistically to induce LTP during theta-burst stimulation (Fig. 2; see also ref. 6). This can be attributed to the ability of each of these channels to produce depolarization and voltage-dependent calcium influx[24]. The occurrence of LTP in the presence of NMDA receptor antagonists suggests that NMDA receptor activation facilitates this form of LTP, but is not required. The persistence of dendritic spikes and LTP during partial block of voltage-gated calcium channels suggests that the sodium channels and unblocked calcium channels can act together with AMPA (α-amino-3-hydroxy-5-methyl-4-isoxazole propionic acid) and NMDA receptor activation to induce LTP. NMDA receptor activation may also contribute to the dendritic spikes that enhance LTP[25].

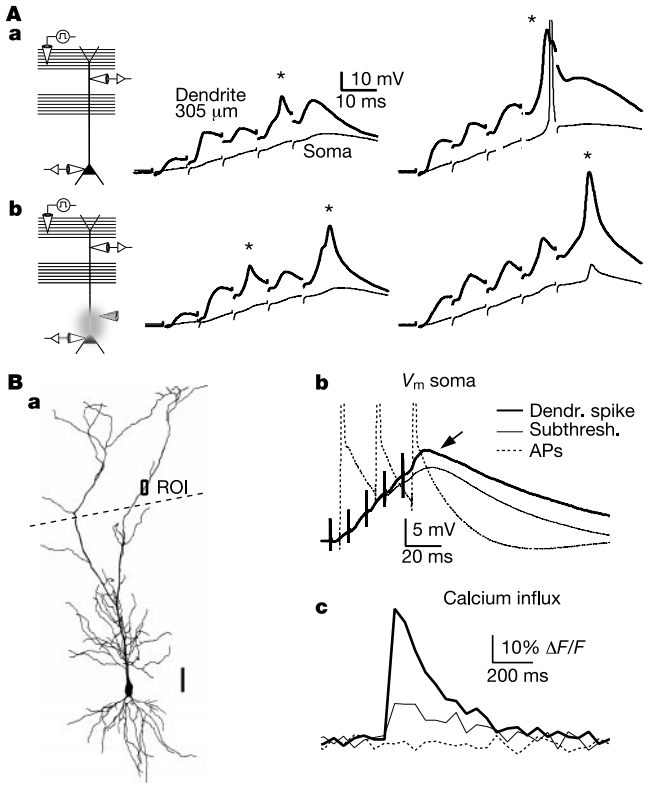


**Figure 3** Large theta-burst responses and distal calcium influx are associated with dendritic spikes. **A,a**, Theta-burst responses recorded simultaneously at the soma and distal dendrite. Dendritic spikes (asterisks) appeared highly attenuated at the soma, and were variably coupled to action potential initiation in the axon. **A,b**, Proximal application of TTX blocked somatic action potentials without affecting dendritic spikes (asterisks) or synaptic potentials. Small spikes at the soma correspond to much larger spikes in the dendrites. **B,a**, Reconstruction of biocytin-labelled neuron used for calcium imaging. Calcium transients were imaged in the SLM, 430 μm from the soma. For clarity, the box indicating the region of interest (ROI) is exaggerated in size. Dotted line indicates the SR/SLM border. Scale bar, 50 μm. **B,b**, The cell was stimulated either with 50 Hz triplets of action potentials (dotted trace) or with single burst synaptic stimuli evoked at intensities just below (thin trace) and above threshold (thick trace) for dendritic spike initiation (detected in the somatic recording as a small spikelet, arrow). **B,c**, Calcium influx (reported by the relative fluorescence change, $\Delta F/F$) in SLM during the three stimuli shown in **B,b**. Dendritic spikes were associated with large calcium transients ($\Delta F/F$, see Methods), whereas backpropagating action potentials and subthreshold theta-burst responses were associated with smaller calcium accumulations.

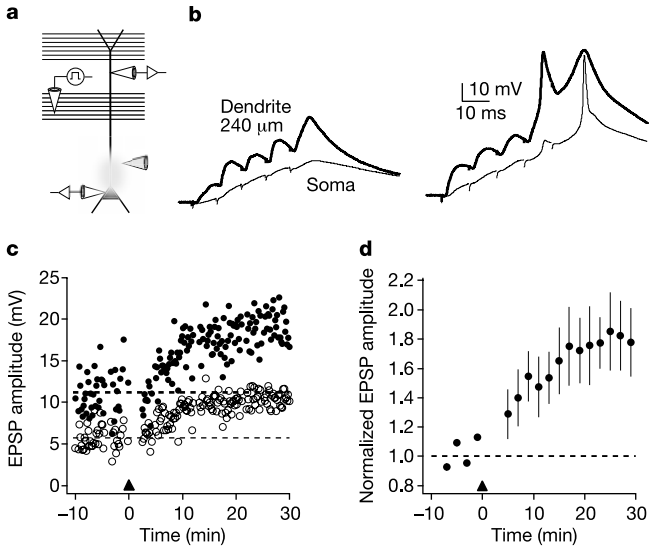


**Figure 4** Dendritic spikes contribute to LTP induction at stratum radiatum (SR) synapses. **a**, Experimental configuration. Responses to SR stimulation were recorded in the dendrites and soma. TTX was applied near the soma during theta-burst stimulation. **b**, Examples of dendritic spikes in response to theta-burst stimulation in SR. Dendritic spikes are strongly attenuated at the soma. **c**, LTP induction at SR synapses can occur independently of backpropagating action potentials. EPSPs measured simultaneously in the dendrite (filled circles) and soma (open circles) before and after theta-burst stimulation in the presence of somatic TTX. **d**, Summary data of dendritic EPSP amplitudes in LTP experiments where backpropagating action potentials were blocked ($n = 4$).

Our findings reveal an important function of dendritically generated spikes. Although these events may contribute to action potential initiation in the axon, their propagation from the dendrites to the soma is limited, both *in vitro* and *in vivo*[9,14–18], suggesting that they may also serve a local function in dendrites. Our data suggest that dendritic spikes can provide the depolarization and calcium entry required for LTP. Although backpropagating action potentials had no effect on theta-burst-induced LTP at SLM synapses, they may be important at these synapses under other conditions. For example, backpropagating action potentials may alter the threshold for dendritic spikes and the extent of their propagation within the dendritic tree[26].

Although we used somatic TTX application or hyperpolarization to prevent action potential initiation and backpropagation during theta-burst stimulation, a similar situation may occur *in vivo* if the soma is inhibited while the dendrites are excited. Indeed, during hippocampal theta rhythm the distal dendrites are excited by glutamate-mediated synaptic potentials, which can trigger dendritic spikes, at a time when the soma is inhibited by GABA-($\gamma$-aminobutyric acid) mediated synaptic potentials[16,27]. Dendritic inhibition may also influence dendritic spikes and LTP. Inhibition that arrives concurrently with excitation would limit dendritic spikes[28], whereas inhibition that arrives before an excitatory input could enhance dendritic spikes by removing inactivation of sodium and calcium channels.

The existence of a form of LTP that does not require action potential output via the axon has implications for plasticity rules and the cellular mechanisms of learning. Whereas synapses located anywhere in the dendrites can cooperate to produce action potentials in the axon and backpropagation-induced LTP, only spatially co-localized synapses are expected to cooperate to produce dendritic-spike-induced LTP. Also, although backpropagating action potentials invade much of the dendritic tree[10], the spread of dendritic spikes is more limited[15,17,19], implying that dendritic spikes will induce LTP at synapses within smaller dendritic domains. The implementation of cooperative LTP[2–5] via dendritic spikes may therefore lead to the selection of clusters of effective synapses in dendritic domains or branches, a property of dendritic integration that has been proposed to increase the computational power and memory capacity of some neural systems[29,30]. □

## Methods

### Hippocampal slice preparation

Transverse hippocampal slices (300 μm) were made from 5–9-week-old Wistar rats as described previously[15]. Dissection and slicing were performed in ice cold, oxygenated (bubbled with 95% $O_2$, 5% $CO_2$) artificial cerebrospinal fluid (ACSF), containing (in mM): 125 NaCl, 2.5 KCl, 2 $CaCl_2$, 1 $MgCl_2$, 25 $NaHCO_3$, 1.25 $NaH_2PO_4$, 25 glucose. Slices were incubated for 30 min in a holding chamber at 35 °C and then stored at room temperature for at least 30 min. Individual slices were then transferred to a submerged recording chamber perfused with ACSF at 35 ± 2 °C. Neurons were visualized with differential interference contrast optics. Synaptic stimulation was achieved with a relatively large (~20 μm diameter) patch pipette connected to a stimulus isolator (Axon Instruments), and placed at least 1 mm from the recorded cell either in SLM or the distal third of SR. All experiments were performed in the presence of the $GABA_A$ and $GABA_B$ receptor antagonists SR95531 (4 μM) and CGP55845A (1 μM), which facilitated activation of dendritic spikes and induction of LTP[4,15,17]. Dendritic spikes could also be elicited with half-maximal block of GABA-mediated transmission (0.44 μM SR95531 and 6 nM CGP55845A), but plasticity was difficult to study owing to contamination of the postsynaptic potential by direct activation of GABA-containing axons (see Supplementary Information).

### Electrophysiology

Whole-cell current-clamp recordings were made from cells in conjunction with bridge amplifiers (Dagan BVC-700). Patch-clamp electrodes were fire-polished and filled with intracellular solution containing (in mM): potassium gluconate 115, KCl 20, sodium phosphocreatine 10, HEPES 10, MgATP 2, NaGTP 0.3, and 0.1% biocytin for subsequent determination of morphology. Electrode resistance in the bath ranged from 2–4 MΩ for somatic and 7–10 MΩ for dendritic pipettes, and series resistance ranged from 9 to 50 MΩ. Electrophysiological traces were digitized via an ITC 16 or ITC18 digital–analog converter (Instrutech) under control of macros custom programmed in IGOR Pro (Wavemetrics).

For LTP experiments, EPSP amplitude was monitored using 0.1-Hz synaptic stimulation. LTP was induced using a theta-burst pairing protocol (Fig. 1). When noted, 5 μM TTX + 0.1% Fast Green dissolved in ACSF was pressure-applied through a patch pipette to the proximal apical dendrite and soma under visual guidance to prevent axonal action potential generation. All other drugs were bath-applied, and present throughout the entire experiment.

### Calcium imaging

In calcium imaging experiments, cells were filled with 150 μM calcium green-1 (Molecular Probes) via the recording electrode for at least 30 min, and excited at 480 nm wavelength. Fluorescence was averaged from small dendritic regions of interest in the SLM (~3 × 10 μm, viewed at 160×), filtered at 535 nm wavelength, and collected with a frame-transfer, cooled CCD camera (EBFT512; Roper Scientific) under the control of custom macros programmed using IGOR Pro. Time-dependent fluorescence changes were background subtracted, and then calculated as $\Delta F/F$, where $\Delta F$ is the time-dependent changes in fluorescence and $F$ is the resting fluorescence. All responses were averages of several trials with a single burst of EPSPs repeated at low frequency (<0.1 Hz). Multiple bursts at theta frequency always evoked larger responses, indicating that the dye was never saturated by a single-burst response.

### Data analysis

Analysis of electrophysiology and imaging data was performed using IGOR Pro Software and statistical tests were performed using Excel software (Microsoft). Statistical analysis of multi-group data was performed using a single-factor analysis of variance. When there was a significant difference between the groups, Tukey's multiple comparison tests were performed to determine the level of significance for each pairwise comparison. All measurements are presented as mean ± s.e.m.

Received 4 April; accepted 9 May 2002; doi:10.1038/nature00854.


1. Hebb, D. O. *Organization of Behavior* (Wiley, New York, 1949).
2. McNaughton, B. L., Douglas, R. M. & Goddard, G. V. Synaptic enhancement in fascia dentata: cooperativity among coactive afferents. *Brain Res.* **157,** 277–293 (1978).
3. Lee, K. S. Cooperativity among afferents for the induction of long-term potentiation in the CA1 region of the hippocampus. *J. Neurosci.* **3,** 1369–1372 (1983).
4. Colbert, C. M. & Levy, W. B. Long-term potentiation of perforant path synapses in hippocampal CA1 in vitro. *Brain Res.* **606,** 87–91 (1993).
5. Sjostrom, P. J., Turrigiano, G. G. & Nelson, S. B. Rate, timing, and cooperativity jointly determine cortical synaptic plasticity. *Neuron* **32,** 1149–1164 (2001).
6. Magee, J. C. & Johnston, D. A synaptically controlled, associative signal for Hebbian plasticity in hippocampal neurons. *Science* **275,** 209–213 (1997).
7. Spruston, N., Schiller, Y., Stuart, G. & Sakmann, B. Activity-dependent action potential invasion and calcium influx into hippocampal CA1 dendrites. *Science* **268,** 297–300 (1995).
8. Callaway, J. C. & Ross, W. N. Frequency-dependent propagation of sodium action potentials in dendrites of hippocampal CA1 pyramidal neurons. *J. Neurophysiol.* **74,** 1395–1403 (1995).
9. Stuart, G., Schiller, J. & Sakmann, B. Action potential initiation and propagation in rat neocortical pyramidal neurons. *J. Physiol.* **505,** 617–632 (1997).
10. Golding, N. L., Kath, W. L. & Spruston, N. Dichotomy of action-potential backpropagation in CA1 pyramidal neuron dendrites. *J. Neurophysiol.* **86,** 2998–3010 (2001).
11. Gustafsson, B., Wigström, H., Abraham, W. C. & Huang, Y.-Y. Long-term potentiation in the hippocampus using depolarizing current pulses as the conditioning stimulus to single volley synaptic potentials. *J. Neurosci.* **7,** 774–780 (1987).
12. Markram, H., Lubke, J., Frotscher, M. & Sakmann, B. Regulation of synaptic efficacy by coincidence of postsynaptic APs and EPSPs. *Science* **275,** 213–215 (1997).
13. Bi, G. Q. & Poo, M. M. Synaptic modifications in cultured hippocampal neurons: dependence on spike timing, synaptic strength, and postsynaptic cell type. *J. Neurosci.* **18,** 10464–10472 (1998).
14. Schiller, J., Schiller, Y., Stuart, G. & Sakmann, B. Calcium action potentials restricted to distal apical dendrites of rat neocortical pyramidal neurons. *J. Physiol.* **505,** 605–616 (1997).
15. Golding, N. L. & Spruston, N. Dendritic sodium spikes are variable triggers of axonal action potentials in hippocampal CA1 pyramidal neurons. *Neuron* **21,** 1189–1200 (1998).
16. Kamondi, A., Acsady, L. & Buzsaki, G. Dendritic spikes are enhanced by cooperative network activity in the intact hippocampus. *J. Neurosci.* **18,** 3919–3928 (1998).
17. Golding, N. L., Jung, H. Y., Mickus, T. & Spruston, N. Dendritic calcium spike initiation and repolarization are controlled by distinct potassium channel subtypes in CA1 pyramidal neurons. *J. Neurosci.* **19,** 8789–8798 (1999).
18. Helmchen, F., Svoboda, K., Denk, W. & Tank, D. W. In vivo dendritic calcium dynamics in deep-layer cortical pyramidal neurons. *Nature Neurosci.* **2,** 989–996 (1999).
19. Häusser, M., Spruston, N. & Stuart, G. J. Diversity and dynamics of dendritic signalling. *Science* **290,** 739–744 (2000).
20. Wei, D. S. *et al.* Compartmentalized and binary behaviour of terminal dendrites in hippocampal pyramidal neurons. *Science* **293,** 2272–2275 (2001).
21. Pike, F. G., Meredith, R. M., Olding, A. W. & Paulsen, O. Postsynaptic bursting is essential for 'Hebbian' induction of associative long-term potentiation at excitatory synapses in rat hippocampus. *J. Physiol.* **518,** 571–576 (1999).
22. Spruston, N., Jaffe, D. B. & Johnston, D. Dendritic attenuation of synaptic potentials and currents: the role of passive membrane properties. *Trends Neurosci.* **17,** 161–166 (1994).
23. Segev, I. & Rall, W. Excitable dendrites and spines: earlier theoretical insights elucidate recent direct observations. *Trends Neurosci.* **21,** 453–460 (1998).
24. Schiller, J., Schiller, Y. & Clapham, D. E. NMDA receptors amplify calcium influx into dendritic spines during associative pre- and postsynaptic activation. *Nature Neurosci.* **1,** 114–118 (1998).
25. Schiller, J., Major, G., Koester, H. J. & Schiller, Y. NMDA spikes in basal dendrites of cortical pyramidal neurons. *Nature* **404,** 285–289 (2000).
26. Larkum, M. E., Zhu, J. J. & Sakmann, B. A new cellular mechanism for coupling inputs arriving at different cortical layers. *Nature* **398,** 338–341 (1999).
27. Kamondi, A., Acsady, L., Wang, X. J. & Buzsaki, G. Theta oscillations in somata and dendrites of hippocampal pyramidal cells in vivo: activity-dependent phase-precession of action potentials. *Hippocampus* **8,** 244–261 (1998).

28. Miles, R., Toth, K., Gulyas, A. I., Hajos, N. & Freund, T. F. Differences between somatic and dendritic inhibition in the hippocampus. *Neuron* **16,** 815–823 (1996).
29. Mel, B. W. Synaptic integration in an excitable dendritic tree. *J. Neurophysiol.* **70,** 1086–1101 (1993).
30. Poirazi, P. & Mel, B. W. Impact of active dendrites and structural plasticity on the memory capacity of neural tissue. *Neuron* **29,** 779–796 (2001).

**Supplementary Information** accompanies the paper on *Nature*'s website (http://www.nature.com/nature).

**Acknowledgements**
This work was supported by the National Institutes of Health.

**Competing interests statement**
The authors declare that they have no competing financial interests.

Correspondence and requests for materials should be addressed to N.S. (e-mail: spruston@northwestern.edu).

# Identification of genes expressed in *C. elegans* touch receptor neurons

**Yun Zhang*, Charles Ma*, Thomas Delohery†‡, Brian Nasipak*, Barrett C. Foat*, Alexander Bounoutas*, Harmen J. Bussemaker*, Stuart K. Kim§ & Martin Chalfie***

* *Department of Biological Sciences, Columbia University, New York, New York 10027, USA*
† *Memorial Sloan Kettering Institute, New York, New York 10021, USA*
§ *Department of Developmental Biology and Genetics, Stanford University Medical Center, Stanford, California 94305, USA*

**The extent of gene regulation in cell differentiation is poorly understood. We previously used saturation mutagenesis to identify 18 genes that are needed for the development and function of a single type of sensory neuron—the touch receptor neuron for gentle touch in *Caenorhabditis elegans*[1,2]. One of these genes, *mec-3*, encodes a transcription factor that controls touch receptor differentiation[3,4]. By culturing and isolating wild-type and *mec-3* mutant cells from embryos and applying their amplified RNA to DNA microarrays, here we have identified genes that are known to be expressed in touch receptors, a previously uncloned gene (*mec-17*) that is needed for maintaining touch receptor differentiation[2,5], and more than 50 previously unknown *mec-3*-dependent genes. These genes are randomly distributed in the genome and under-represented both for genes that are co-expressed in operons and for multiple members of gene families. Using regions 5′ of the start codon of the first 20 genes, we have also identified an over-represented heptanucleotide, AATGCAT, that is needed for the expression of touch receptor genes[6].**

Through mutagenesis screens for touch-insensitive mutants[1,2], we previously identified *mec-3*, *mec-17* and eight *mec-3*-dependent genes that are needed for the function of the six touch receptor neurons (refs 7, 8; and G. Gu, L. Emtage and M.C., unpublished data). Those screens identified several alleles for each of these genes (except *mec-17*) and were therefore at or near saturation; however, they would not have identified genes whose activity is redundant, subtle or pleiotropic, or genes whose loss produces touch-supersensitive animals.

Because adult animals contain roughly 3,000 nuclei but only six touch receptor neurons, the identification of differences in RNA from animals with and without these cells on DNA microarrays has an inherent problem of sensitivity. Indeed, we could not identify any touch receptor genes using RNA from wild-type and *mec-3* mutant animals on DNA microarrays (data not shown). We therefore obtained and cultured wild-type and *mec-3* mutant cells from embryos, isolated touch receptors by cell sorting, and amplified RNA from the isolated cells. We identified the cells by green fluorescent protein (GFP) fluorescence, which was expressed either from the promoter for *mec-18*, a touch-receptor-specific gene, in wild-type embryonic touch receptors (ALML/R and PLML/R), or from the *mec-3* promoter, which is specific to touch receptors and two other neurons (FLPL/R) in the embryo[4], for *mec-3* mutant cells. Both promoters are expressed after the touch receptors are generated.

When initially dissociated, embryos produced a few faintly fluorescent cells. When cultured overnight, however, more cells (0.3–0.6%) elaborated processes and had intense GFP fluorescence. These GFP-positive cells, which were presumably generated and/or differentiated in culture, were similar in morphology (Fig. 1a) and gene expression (Fig. 1b and Table 1) to *in vivo* touch receptor neurons. The wild-type cultured cells were usually monopolar with a single long process or bipolar with a smaller second process at 180° from the first, in other words, they were similar to *in vivo* ALM or PLM cells, respectively. In contrast, the *mec-3* cells were bipolar or multipolar with smaller processes that branched more randomly.

To characterize gene expression in wild-type and mutant touch receptors, we isolated the cells by size, viability and GFP fluorescence intensity using fluorescence-activated cell sorting. A typical sorting produced $4 \times 10^6$ cells, 40–60% of which were GFP positive (~100-fold enrichment). From these cells, we obtained about 100 pg of poly(A)$^+$ RNA, which was amplified linearly by roughly one million times. All nine known *mec-3*-dependent *mec* genes were expressed at much higher levels in wild-type cells than in *mec-3* cells (Fig. 1b and Table 1). (*mec-3* is least differentially expressed probably because of its autoregulation; its expression declines in *mec-3* mutants as animals mature[4]; therefore, the reduction of *mec-3* messenger RNA in embryonic cells was probably not complete.) These results show that the differentiated touch receptors in culture express *mec-3*-dependent genes and that linear amplification can successfully amplify the corresponding RNAs.

To identify *mec-3*-dependent genes, we hybridized RNA from sorted wild-type cells and *mec-3* cells to genomic DNA microarrays containing DNA for 17,817 of the 18,967 known or predicted *C. elegans* genes[9]. Three sets of independently prepared RNA samples from mutant and wild-type touch receptors were each hybridized onto two separate arrays. We identified 71 *mec-3*-dependent candi-

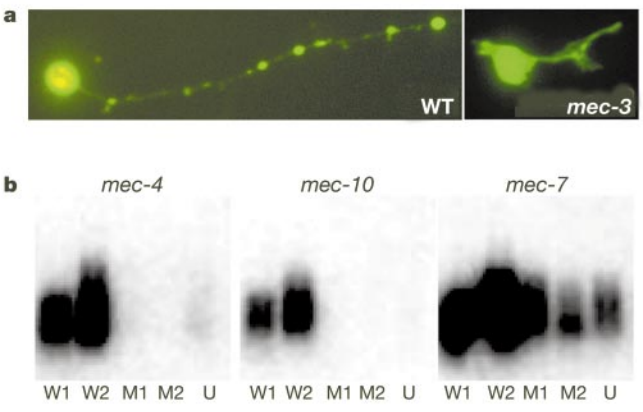


**Figure 1** Morphology and gene expression of cultured *C. elegans* cells. **a**, A wild-type (WT) touch receptor neuron and a *mec-3* mutant cell after 12 h in culture. Both cells fluoresce because of expressed GFP. The wild-type cell has a single neurite, whereas the *mec-3* cell has several shorter neurites. **b**, Northern analyses of amplified RNA from sorted wild-type touch receptors (W1 and W2), sorted *mec-3* mutant cells (M1 and M2), and unsorted wild-type cells (U). Samples were probed with cDNAs for the indicated genes.

‡ Present address: Aventis Pharmaceuticals, 1041 Rt. 202-206, Bridgewater, New Jersey 08807-0800, USA.